Cellulose (2024) 31:6797–6813
https://doi.org/10.1007/s10570-024-05966-x

ORIGINAL RESEARCH

Synthesis of bio-based phosphorus-nitrogen hybrid cellulose nanocrystal flame retardant for improving of fire safety of epoxy resin

Weihua Meng · Chang Wang · Hang Di · Shuo Ren · Jianing Wu · Xuyang Sun · Lide Fang · Xiangjie Kong · Jianzhong Xu

Received: 13 December 2023 / Accepted: 20 May 2024 / Published online: 22 June 2024

Abstract Bio-based materials as flame retardants meet the requirements of green strategy and sustainable development. Here nitrogen and phosphorus-modified bio-based cellulose nanocrystal composite (NPCNCs) were designed and added to epoxy resin (EP) to determine fire safety and mechanical properties. NPCNCs were successfully synthesized using ice bath polymerization and exhibited a fibrous appearance with rough surface. When corresponding into EP, NPCNCs endowed EP composite with excellent flame retardancy. For EP/6NPCNCs, the LOI value was 27.6% which was higher than that of pure EP (23.5%). Compared with pure EP, the total heat release, peak heat release rate, total smoke production and peak smoke production rate values of EP/6NPCNCs decreased by 27.27%, 43.34%, 70.21% and 66.67%. This was attributed to catalysis-dehydration and carbonization, carbon support of cellulose nanocrystals and gas phase dilution. In addition, the flame retardant EP composite mechanical properties were basically maintained compared with the pure EP. This article will provide a new way for the design bio-based P and N-modified flame retardants.

Keywords Epoxy resin · Flame retardant · Cellulose nanocrystal · P/N-modified hybrid

W. Meng (✉) · C. Wang · S. Ren · X. Sun · L. Fang · X. Kong
College of Quality and Technical Supervision, Hebei University, Baoding 071002, China
e-mail: mengweihua121@163.com

W. Meng · S. Ren · X. Sun · L. Fang · X. Kong
Engineering Research Center of Zero Carbon Energy Building and Measurement Technology, Ministry of Education, National & Local Joint Engineering Research Center of Metrology Instrument and System, Hebei University, Baoding 071002, China

W. Meng
Fujian Key Laboratory of Special Intelligent Equipment Safety Measurement and Control, Fujian Special Equipment Inspection and Research Institute, Fuzhou 350008, China

W. Meng · C. Wang · H. Di · S. Ren · J. Wu · J. Xu
College of Chemistry and Materials Science, Hebei University, Baoding 071002, China

Introduction

Epoxy resins (EP) are widely used in automotive, electrical, aerospace and other fields (Qi et al. 2023) for advantages of stable structure, good heat resistance and excellent mechanical properties. However, the EP's inherent flammability results in high fire risk during the real application, which restricted the application (Huo et al. 2021). Therefore, flame retardant modification was particularly important for EP (Zhou et al. 2017). Adding flame retardants was an important flame retardant modification method (Zhi et al. 2022).

Intumescent flame retardant was one of the most important additive flame retardants, which was formed by acid source, carbon source, and gas source. Due to the synergistic effect of catalytic carbonization (Chen and Wang 2010), free radical scavenging (Luo et al. 2020) and gas phase dilution (Peng et al. 2021), intumescent flame retardants showed excellent flame retardancy. In recent years, a series of green and renewable biomass materials, such as cellulose, chitosan, lignin, starch and phytic acid (PA), had been used to construct intumescent flame-retardant system (He et al. 2022; Zhi et al. 2022).

Cellulose nanocrystals (CNCs) were nanorods extracted from natural cellulose, which were important flame retardant biomaterials due to their excellent properties such as high crystallinity, high strength, high elastic modulus, biodegradability, and abundant surface active sites (Zhou et al. 2017). CNC@MEL-PA was prepared from MEL, PA and CNCs to achieve good thermal stability, char forming properties, and effective flame retardancy (Zhang et al. 2023). FCNC hybrid materials was synthesized by functionalizing CNCs using silane coupling agents and 9,10-dihydro-9-oxa-10-phospha-phenanthrene-10-oxide (DOPO) (Du et al. 2022), which can effectively improve waterborne polyurethane's flame retardancy and mechanical properties. CNC@DPP@Zn was prepared using esterification and transition metal chelation (Suo et al. 2022), when used in EP it formed a continuous and dense cross-linked composite. When thermal degradation, CNCs could form a continuous and dense cross-linked char layer under the synergistic effect with other flame retardants (He et al. 2022; Zhang et al. 2020), while reducing heat release and smoke release. Also, as a green natural polymer material, CNCs had broad application prospects in green flame-retardant systems due to their rich carbon content and high active sites.

PA was a green dehydrating agent from grains, legumes and other plants with higher phosphorus content, which exhibited excellent char-forming effect during combustion and synergistic flame retardancy (Meng et al. 2020; Mokhena et al. 2022). Phytic acid doped polyaniline nitride carbon nanosheets were synthesized to effectively improve the "candle core effect" of cotton and polyester during thermal decomposition (Chen et al. 2023a, b). Chitosan/phytate was deposited onto the surface of polyester/cotton blended fabrics by layer-by-layer self-assembly to construct a bio-based intumescent flame-retardant system (Fang et al. 2021). When the deposition reached 20 layers, the LOI value of the blended fabric was 29.2% and the melting droplet phenomenon of the fabric disappeared. A novel intumescent flame retardant PAD was prepared by combining PA with DOPO, and the EP/5 wt% PAD showed obvious intumescent behavior (Yang et al. 2022).

Polyaniline (PANI) is a typical nitrogen-containing polymer compound. Because of good compatibility, simple synthesis process, good physical and chemical stability, and good processability, PANI has been widely used in the flame retardant field (Li et al. 2014). A multifunctional coating containing graphene oxide and PANI on the surface of cotton fabric was constructed through in-situ polymerization and spray-assisted layer-by-layer assembly (Zeng et al. 2021). The coating played the molecular interaction between different layers and the synergistic effect of different elements to entrust cotton fabric with excellent self-extinguishing and flame retardancy. A non-carbonized nanostructured aerogel was developed by a top-down approach, which had electromagnetic interference shielding, flame retardancy and photothermal conversion capabilities (Chen et al. 2021).

In this paper, a novel CNC-based intumescent flame retardant was constructed to use PA and aniline as raw materials and utilizing the surface-active sites of CNCs. Then it was applied to EP to study the flame retardant, mechanical properties, and the possible flame retardant mechanisms were revealed by analyzing the carbon residue in condensed phase and the pyrolysis products in gas phase.

Experimental

Materials

Cellulose nanocrystals (CNCs) were provided by Huzhou Sansi New Material Technology Co., Ltd.. Aniline (> 99.5%) and ammonium persulfate (APS, > 98%) were purchased from Tianjin Fuchen Chemical Reagent Factory. Phytic acid (PA, 50%) was obtained from Shanghai Aladdin Biochemical Technology Co., Ltd.. M-phenylenediamine were offered by Shanghai MacLean Biochemical Technology Co., Ltd. EP resin (E-44) was offered by Sinopec Group Asset Management Co., Ltd.. All reagents were of

analytical grade and can be used directly without further processing.

Preparation of NPCNCs

NPCNCs was successfully prepared by ice bath polymerization and the detail procedure was as follows. 0.625 g of aniline was added to 100 mL H_2O and dispersed for 30 min. Then, 5.5 g of PA was added to the above solution and mixed uniformly, and then the suspension of CNCs (1.56 wt%, 10.26 g) was dropped into the above-mixed solution, and then ultrasonically treated for 100 min to make the aniline monomer self-assemble on the surface of CNCs. Finally, 0.76 g of APS was added to the mixture under mechanical agitation and polymerized in an ice bath for 3 h. After centrifugation, washed with water, and dried, the dark green product was obtained which was denoted as NPCNCs.

Preparation of EP/NPCNC composites

The preparation method of the EP composite was as follows: First, 100 g EP was placed in a suction filter bottle, then placed in a water bath under 60 °C, and the air bubbles in the system were removed. Afterward, 3.0 g CNCs, 3.0 g NPCNCs, 6.0 g NPCNCs and 9.0 g NPCNCs were added to the EP, and stirred to fully disperse, respectively. Then, 11.0 g curing agent m-phenylenediamine was added into the above mixture. After dispersed evenly, the mixed composite was quickly poured under the preheated Teflon mold. Finally, it was transferred to a vacuum oven to cure at 80 °C for 2 h and recure at 150 °C for 3 h. The samples were noted as EP/3CNCs, EP/3NPCNCs, EP/6NPCNCs, and EP/9NPCNCs, respectively. In comparison, pure EP was prepared in the same method without flame retardant being added.

Characterization

The morphology was characterized by a scanning electron microscope and energy dispersive X-ray spectrometry (SEM–EDS, TM4000, Japan), using an accelerating voltage of 15 kV and gold spraying under a vacuum to increase the conductivity before testing. At the same time, the content of various elements was determined by spectral line scan and spectral surface scan (mapping). Also, transmission electron microscopy (TEM, Tecnai G2 F20 S-TWIN, USA, accelerating voltage of 200 kV) was used to characterized the morphology.

The chemical bonding mode of the composites was studied using Fourier transforms infrared spectroscopy (FTIR, TENSOR 27, Bruker, Germany) and X-ray photoelectron spectroscopy (XPS, Escalab 250Xi, Thermo Scientific, America). FTIR used the KBr pellet technique in the range of 4000–400 cm^{-1}. XPS used Al Kα excitation radiation ($h\nu = 1486.6$ eV) collected in the process.

The structure of the material was characterized by X-ray diffraction (XRD, D8-ADVANCE, Bruker, Germany) on the sample powder in the scanning range of 5–60° with a scanning speed of 0.1 s/0.02° and Cu Kα radiation at 40 kV.

The thermal stability was analyzed using a thermogravimetric analyzer (TGA, STA449C, NETZSCH, Germany) under nitrogen and air conditions. The temperature was raised from room temperature to 800 °C at a heating rate of 10 °C/min.

The limiting oxygen index (LOI) was tested on the HC-2 oxygen index meter (PX-05–005) using the GB/T2567-2008 test standard. The size of the sample tested is $130 \times 6.5 \times 3.2$ mm^3. The combustion behavior of the material was tested using a cone calorimeter (CCT, iCONE plus, Fire Testing Technology, UK) according to the ISO 5660 test standard. A sample of $100 \times 100 \times 3$ mm^3 was covered with aluminum foil, and the combustion test was carried out at a heat flux of 50 kW/m^2.

Raman spectroscopy was performed on the 532 nm laser of the LabRAM HR Evolution Raman spectrometer. Generally, each carbon residue sample was collected from three locations, with a test range of 800–2000 cm^{-1}.

The tensile strength was measured by an electronic universal testing machine (UTM4204, SUNS, China). The splines were $100 \times 5 \times 3$ mm^3 in size according to the GB/T2567-2008 standard, and the tensile speed was 50 mm/min. The impact strength was measured using a pendulum impact tester (ZBC2000-B, Winters Industrial Systems) with an impact bar size of $60 \times 4 \times 10$ mm^3. The test specimens for mechanical properties were all five, and the final data was the average of the five samples.

Thermogravimetric analysis and Fourier transform infrared spectroscopy (TG-FTIR) were performed on the composites using an FTIR

spectrometer (USA-Thermo Fisher-IS50 Infrared) and a TGA2 thermogravimetric analyzer (Mettler, Switzerland) under nitrogen atmosphere. About 5.0 mg of the sample was heated from room temperature to 800 °C at a heating rate of 10 °C/min.

Results and discussions

Characterization of NPCNCs

The morphology of prepared flame retardant was characterized by TEM (Fig. 1(a-b)). The CNCs presented a fibrous structure with a length of about 200 nm and a diameter of about 20 nm. NPCNCs also presented fibrous structure coated with spheres which was the phosphorous nitrogen containing materials. The EDS and mapping results showed that NPCNCs were composed of C, O, N and P elements and these elements were uniformly dispersed in the prepared material. The XRD patterns of CNCs showed a broad peak at 15.6°/16.5°, 22.5°and 34.6°, which were attributed to the overlapped peaks from the (1-10) and (110) planes, to the (200) planes, and to the (004) planes, respectively, characteristic of cellulose I. Also, the peak at 25.2° appeared and the peaks of the NPCNCs were reduced, indicating the P and N modification reduced the degree of crystallization.

As shown in the FTIR spectra (Fig. 1(e)), CNCs showed typical absorption bands ~ 3414 cm^{-1} (-OH stretching vibration), 2900 cm^{-1} (-CH stretching vibration), 1633 cm^{-1} (absorbed water), 1435 cm^{-1}, 1382–1375 cm^{-1} (C-H bending), 1335–1315 cm^{-1} (O–H bending and CH_2 wagging), 1278–1285 cm^{-1}, 1155 cm^{-1} (C–C stretching in ring structure), 1113 cm^{-1} (C–O–C glycosidic ether), and 1054 cm^{-1} (C–O–C stretching in pyranose ring), 902–894 cm^{-1} (glycosidic linkages) (Kumar et al. 2017). For PANI, there were signals corresponding to quinoid, benzenoid ring, and N–H vibrations at 1555, 1479, and 1299 cm^{-1}, respectively (Li et al. 2014). The characteristic bands in NPCNCs were red-shifted to 1545, 1478 and 1297 cm^{-1}, respectively, indicating a strong interfacial interaction between CNCs and PANI. In addition, new absorption bands appeared at 551 and 798 cm^{-1}, representing the symmetry vibration of P-O-C and the stretching vibration of P = O, respectively, which was the result of the protonation effect between PA and PANI (Huang et al. 2021).

The elements and bonding modes of CNCs and NPCNCs were characterized by XPS. According to Fig. 2, CNCs had typical peaks C and O. While in NPCNCs, the existence of N and P elements could be

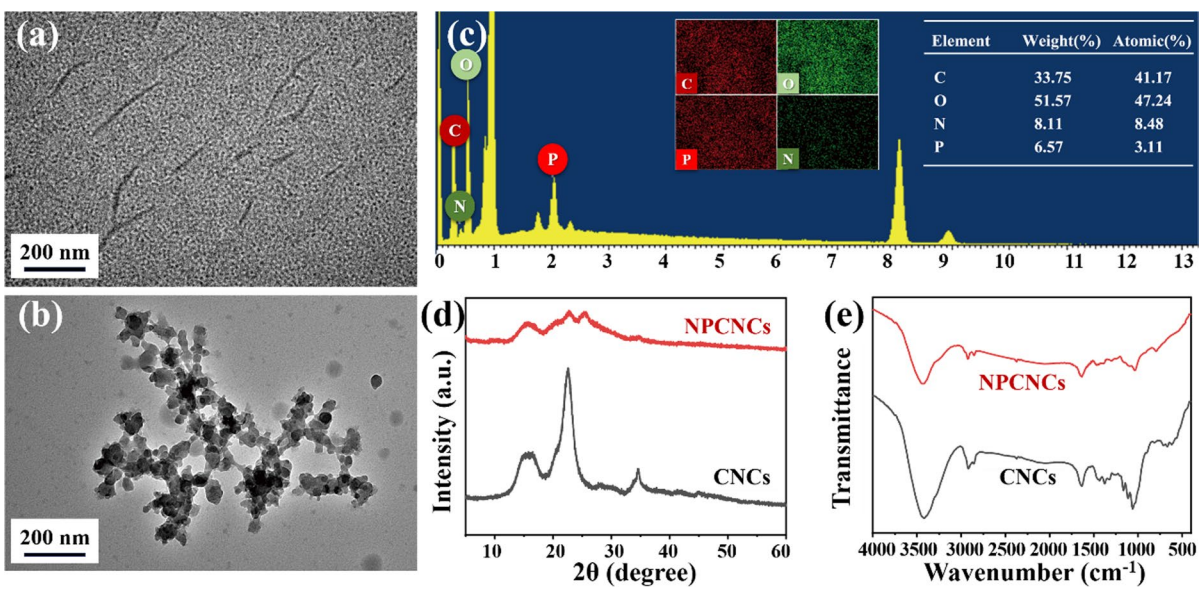

Fig. 1 TEM image of (**a**) CNCs and (**b**) NPCNCs; (**c**) the element mappings and EDS for NPCNCs; (**d**) XRD patterns and (**e**) FTIR spectra

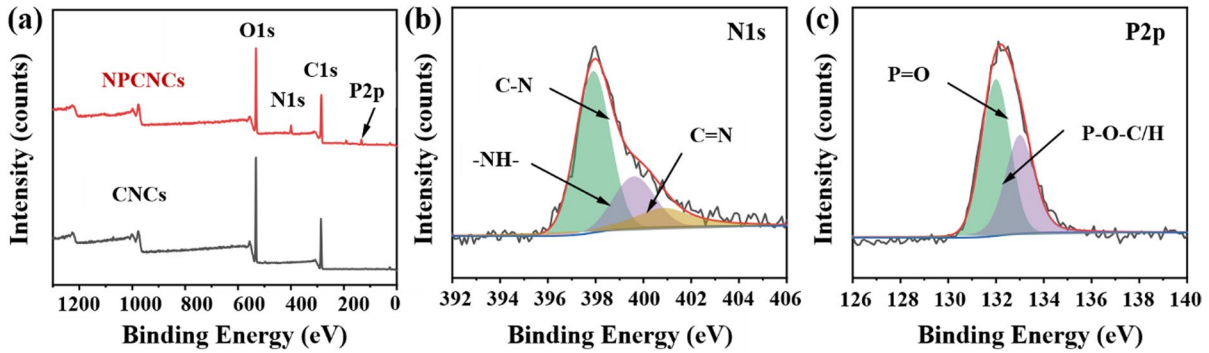

Fig. 2 **a**) XPS spectra of CNCs and NPCNCs, high-resolution (**b**) N 1 s and (**c**) P 2p XPS spectra of NPCNCs

observed. In addition, the peaks of N1s and P2p spectra of NPCNCs were divided. There were three peaks in N1s spectrum, corresponding to C-N (397.9 eV), -NH- (399.6 eV) and C = N (400.83 eV) (Bhoite et al. 2021). The P2p spectrum contained two peaks corresponding to P = O (132.7 eV) and P-O-C/H (133.4 eV) (Cheng et al. 2021). These results indicated that the synthesis of NPCNCs was successful.

In order to study the thermal stability, CNCs and NPCNCs were analyzed using TGA in N_2 atmosphere. Figure 3(a) showed that there were two degradation stages in CNCs: the first stage (below 150 °C) was related to the evaporation of free water; The second stage occurred at around 220–350 °C with the dehydration of the sugar ring and the breaking of the C–O–C bond of the glycoside (He et al. 2022). NPCNCs had a similar decomposition stage with CNCs. The initial decomposition temperature ($T_{5\%}$) of NPCNCs was decreased from 253.9 °C ($T_{5\%}$ of CNCs) to 125.0 °C, indicating that the addition of phytic acid and aniline promoted the decomposition in advance. The maximum mass loss rate (R_{max})

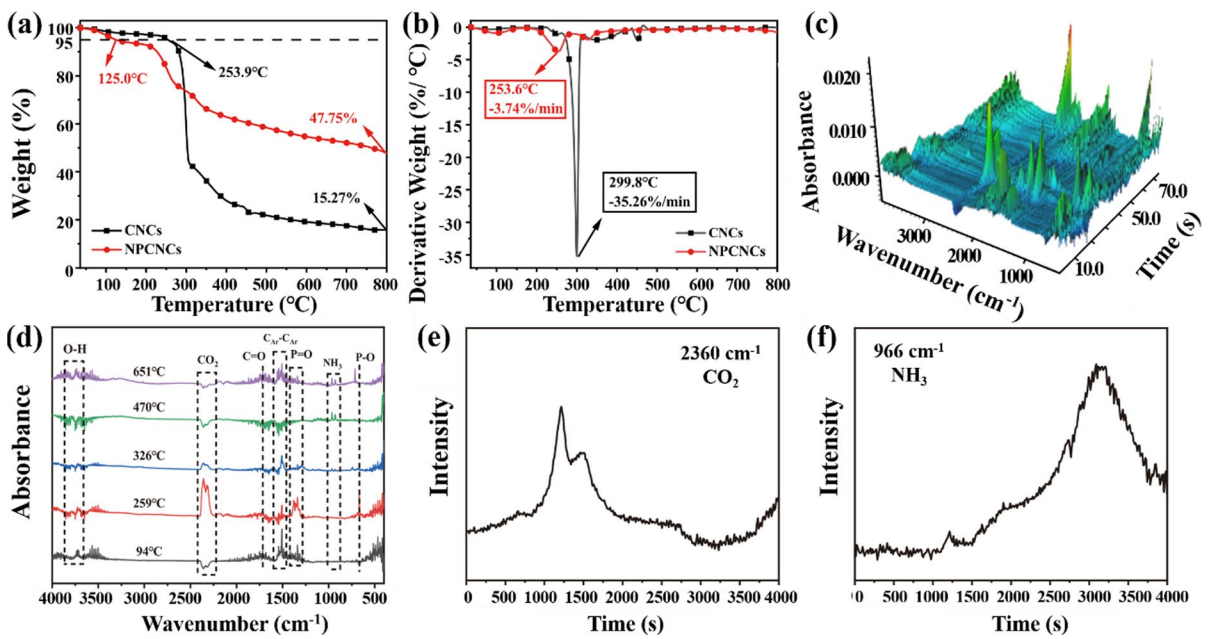

Fig. 3 **a**) TGA and (**b**) DTG curves of CNCs and NPCNCs in N_2 atmosphere. (**c**) 3D TG-FTIR spectra; (**d**) FTIR spectra of the pyrolysis products at different temperature; the (**e**) CO_2 and (**f**) NH_3 release trajectory over time of NPCNCs

of NPCNCs was reduced to 3.74%/min, compared with that of CNCs (35.26%/min). And at 800 °C, the residual mass of CNCs and NPCNCs were 15.72% and 47.75%, respectively. The results showed that the NPCNCs have excellent char forming ability, which can provide an effective physical barrier to isolate heat, smoke, and combustible gases, thereby inhibiting mass and heat transfer during the combustion process.

The pyrolysis products of NPCNCs during thermal decomposition were evaluated by TGA-FTIR. According to 3D spectra and the FTIR spectra at different temperature (Fig. 3(c-d)), the bands of O–H (3710–3850 cm^{-1}) and C_{Ar}-C_{Ar} (1480–1570 cm^{-1}) appeared (Peng et al. 2021) at the first degradation process, and the production of CO_2 (2360 cm^{-1}), P = O (1305–1400 cm^{-1}), P-O-C (669 cm^{-1}) and NH_3 (929 and 966 cm^{-1}) appeared at the second degradation process (Fang et al. 2020; Wang et al. 2023a, b). The phosphorous groups can capture H· and OH· active radicals, terminate the chain combustion reaction, and prevent the combustion in the gas phase (Xiao et al. 2023). CO_2 and NH_3 was nonflammable gases that can dilute oxygen and gaseous combustible products, resulting in combustion discontinuation (Peng et al. 2021).

Thermal behavior of prepared composites

The TGA and derivative thermogravimetry (DTG) curves of EP composites under N_2 and air atmosphere was shown in Fig. 4, and the relevant data were listed in Table 1. As can be seen under N_2 atmosphere, both pure EP and the flame-retardant EP composites exhibited only one degradation process (300–400 °C), which was mainly caused by the molecular chains fracture of EP (Kandola et al. 2022). For pure EP, the $T_{5\%}$ was 361.4 °C, the R_{max} was -18.09%/min at 376.5 °C (T_{max}), and the residual char was 14.22% at 800 °C. The flame-retardant EP composites exhibited similar pyrolysis behavior. And with the addition amount increasing, the $T_{5\%}$ and T_{max} value decreased more obviously. In addition, the residual char of EP/9NPCNCs reached 25.00%, which was 75.8% higher than that of pure EP. The results showed that the addition of NPCNCs promoted the early degradation of EP composites and the formation of char layers.

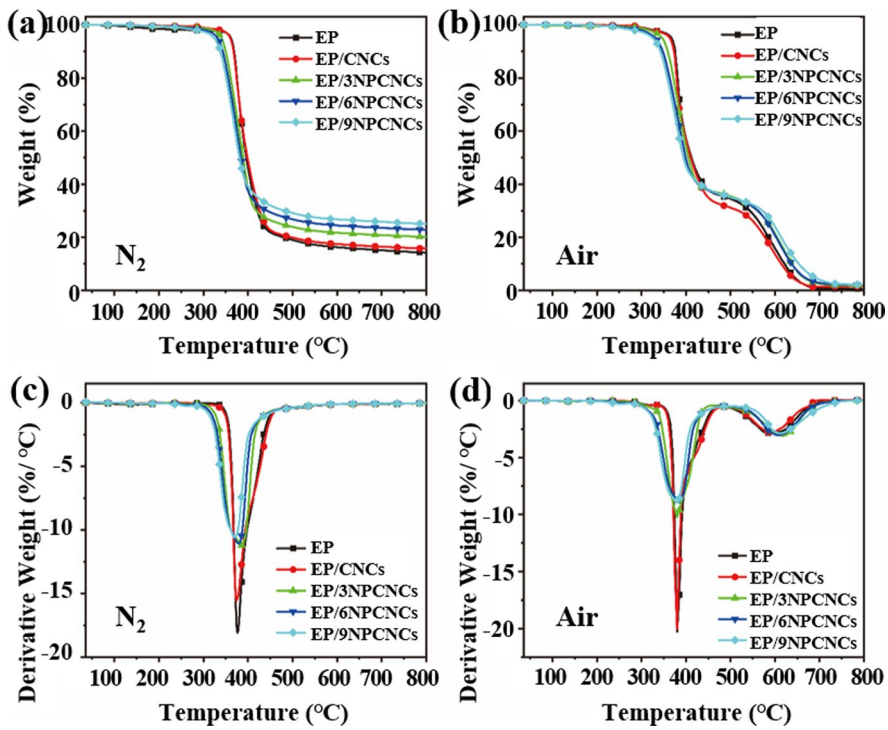

Fig. 4 **A**-**b**) TGA and (**c**-**d**) DTG curves of EP composites

Table 1 Thermal decomposition data of EP composites

Atmosphere	Samples	$T_{5\%}$ (°C)	T_{max} (°C)	R_{max} (%/min)	$Char_{800°C}$ (%)
N_2	EP	361.4	376.5	-18.09	14.22
	EP/3CNCs	360.1	374.4	-15.57	15.79
	EP/3NPCNCs	340.1	384.1	-11.25	20.19
	EP/6NPCNCs	331.5	379.1	-11.10	22.83
	EP/9NPCNCs	323.8	369.5	-10.59	25.00
Air	EP	367.8	380.9	-20.54	0.79
	EP/3CNCs	364.1	379.1	-20.10	1.63
	EP/3NPCNCs	346.5	380.2	-10.26	1.97
	EP/6NPCNCs	331.3	387.3	-8.67	2.14
	EP/9NPCNCs	325.3	379.3	-8.98	2.20

Under air atmosphere, there were two degradation stages for pure EP and EP composites: the first degradation stage was about the molecular chains fracture of EP; the second stage (500–700 °C) was corresponded to the degradation of residual char (Feng et al. 2018). At the second stage, compared with pure EP, the EP/NPCNCs degradation temperature increased and decomposition rate slowed down, both showing that the addition of NPCNCs can significantly improve the thermal oxidation stability of residual char, then improving the fire resistance of EP (Xiao et al. 2023).

Flame retardancy tests

The limiting oxygen index (LOI) is the minimum concentration that supports the combustion of a material to describe the flame retardancy (Chen et al. 2023a, b). The LOI values of pure EP and EP/3CNCs were 23.5% and 23.0%, respectively, indicating that both were extremely flammable. The LOI values of EP/3NPCNCs, EP/6NPCNCs, and EP/9NPCNCs were 27.0%, 27.6%, and 26.7%, respectively, indicating that NPCNCs can improve the flame retardancy of EP and reduce fire risk.

Cone calorimetry (CCT) is an effective method to measure the combustion performance, and can provide some important parameters (Lou et al. 2023). The related data results were shown in Table 2 and Fig. 5. As shown in Fig. 5(a-b), pure EP was ignited at 54 s and reached a peak heat release rate (PHRR) (1242.79 kW/m^2) at 125 s, with a total heat release (THR) of 116.35 MJ/m^2. The EP/3CNCs was ignited at 49 s, with a slightly decrease in PHRR value (1242.79 kW/m^2) and in THR (119.73 MJ/m^2). This indicated that CNCs promoted the early degradation of EP materials, but did not play a positive role in the combustion of EP. With the NPCNCs different addition, the ignition time of EP composites was advanced to 39, 42 and 36 s, respectively, indicating that NPCNCs can promote the degradation of EP, which was consistent with the results of TGA. Compared with

Table 2 Correlation data of LOI and cone calorimetry

Samples	EP	EP/3CNCs	EP/3NPCNCs	EP/6NPCNCs	EP/9NPCNCs
LOI (%)	23.5	23.0	27.0	27.6	26.7
TTI (s)	54	49	44	43	40
THR (MJ/m^2)	116.35	119.73	100.23	94.62	95.17
PHRR (kW/m^2)	1242.79	1139.67	892.55	704.11	694.83
Av-EHC (MJ/kg)	29.77	31.55	26.81	27.51	26.91
Av-SEA (m^2/kg)	1079.67	1132.58	1046.23	906.42	769.51
TSP (m^2)	38.91	39.88	33.00	11.59	24.45
PSPR (m^2/kg)	0.39	0.45	0.23	0.13	0.22
t_{PSPR} (s)	120	110	95	110	80
Residue (%)	9.84	7.53	16.59	21.34	20.93

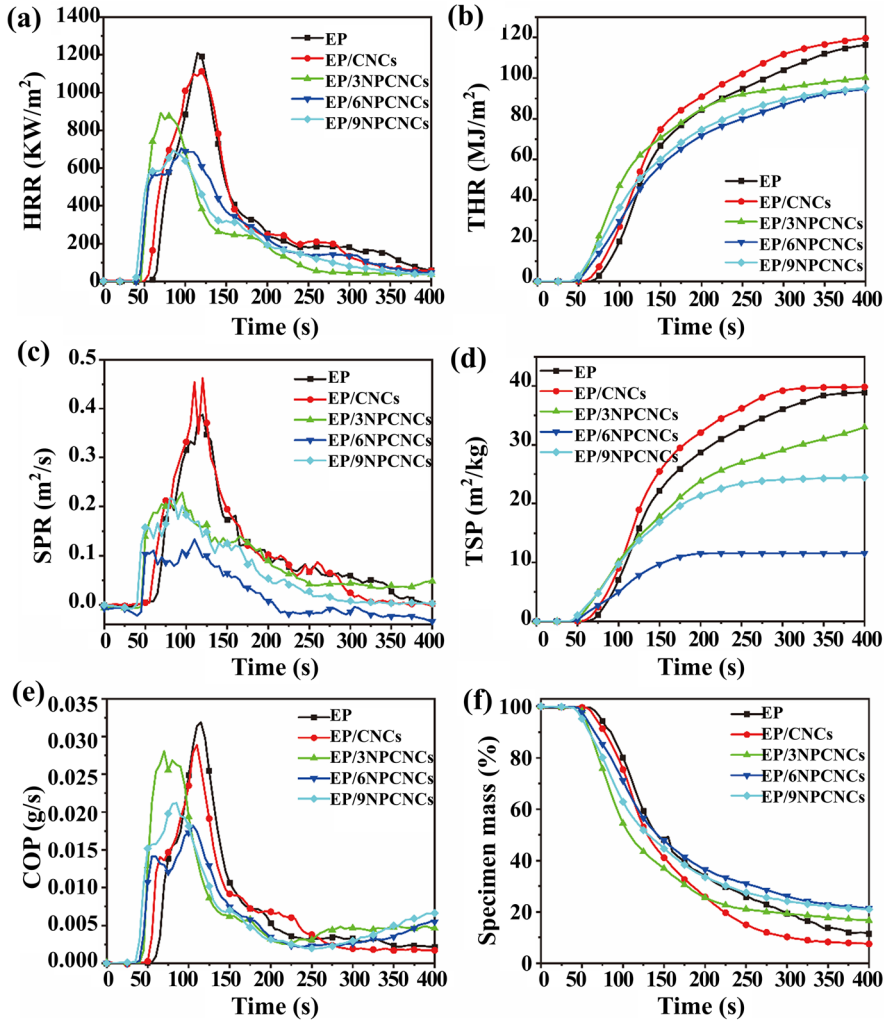

Fig. 5 The related CCT data of EP composites. (**a**) HRR; (**b**) THR; (**c**) SPR; (**d**) TSP; (**e**) COP and (**f**) Mass

pure EP, the THR of EP/3NPCNCs, EP/6NPCNCs, and EP/9NPCNCs decreased by 13.85%, 27.27% and 18.20%, respectively, and the PHRR decreased by 28.18%, 43.34%, and 44.09%, respectively. This may be due to the prepared flame retardant promoting the formation of residual carbon in the matrix during the combustion process, thereby inhibiting the release of heat (Wang et al. 2019).

As shown in Fig. 5(c-d), pure EP released a large amount of smoke during combustion, reaching a peak PSPR of 0.39 m^2/kg at 120 s, and with TSP of 38.91 m^2. The TSP and PSPR of EP/3CNCs slightly increased. While EP/3NPCNCs, EP/6NPCNCs and EP/9NPCNCs reached PSPR of 0.23, 0.13 and 0.22 m^2/kg at 95, 110 and 80 s, respectively. The related TSP value decreased by 15.19%, 70.21%, and 37.16%, respectively. NPCNCs effectively inhibited the generation of smoke during the combustion process of EP composites, improving the fire safety of EP. The decrease in the Av-SEA value of EP/NPCNC composites also clearly confirmed this conclusion. Additionally, the release of CO showed the similar trend of HRR and SPR. The reduction of smoke and toxic gases (CO) can improve the fire safety of EP.

In addition, compared with pure EP, the Av-EHC values of EP/NPCNC composites were all increased, indicating that NPCNCs played a role mainly in the condensed phase (Zhang et al. 2017). During the combustion process, the composite generated a dense expanded char layer, which played a good role in heat and oxygen insulation. Then smoke and solid particles generated during the combustion process need

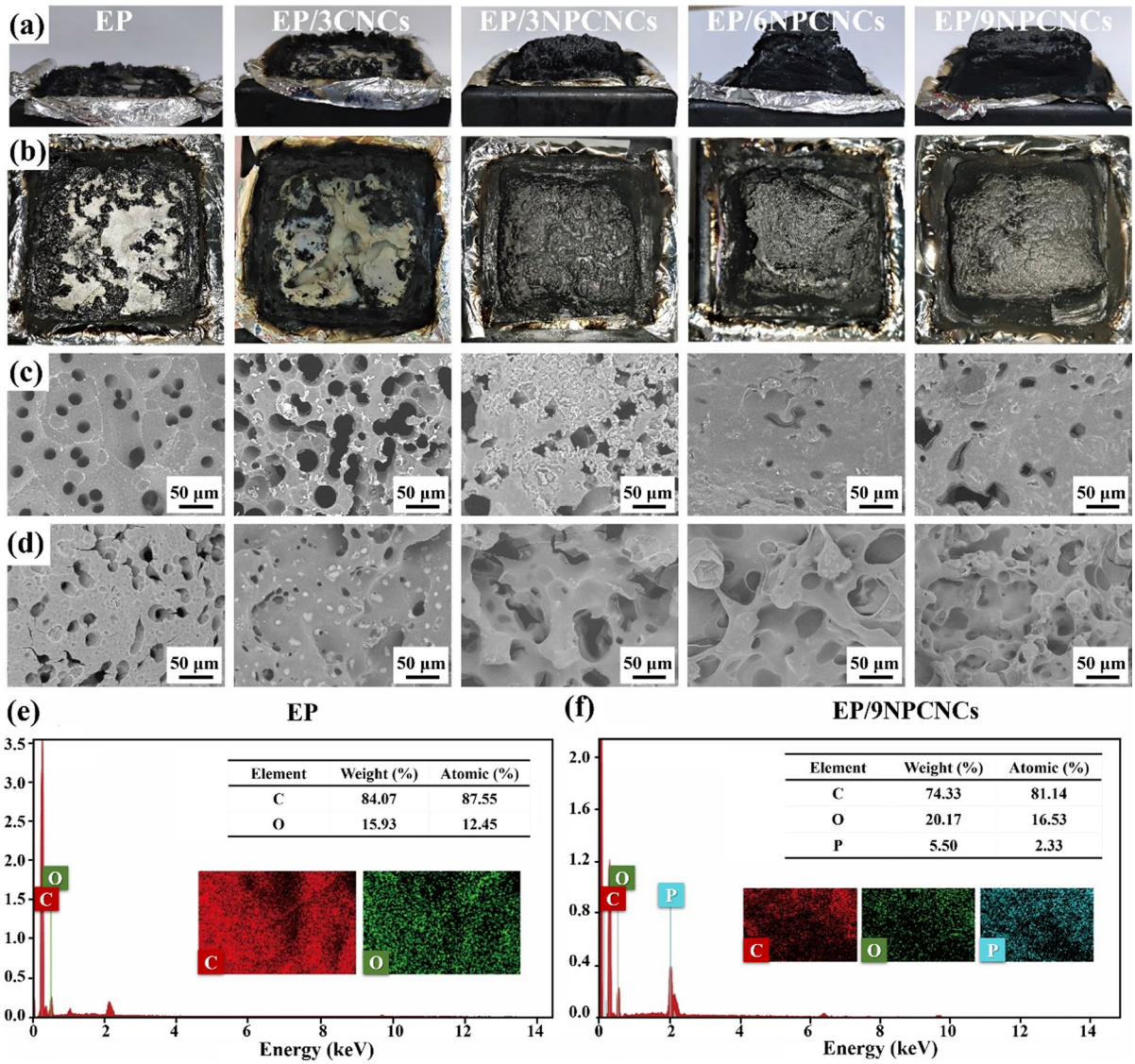

Fig. 6 (**a**–**b**) Digital photos (**c**) SEM of the carbon residue outer surface, (**d**) SEM of carbon residue inner surface, the EDS of (**e**) EP and (**f**) EP/9NPCNCs

to pass through complex pathways to be released into the air, and remained inside the char layer (Meng et al. 2022).

Flame-retardant mechanisms

To study the condensed phase mechanism, the carbon residue after CCT test were characterized using digital camera, SEM, Raman and XRD. In the digital photos, the carbon residue of pure EP was less and broken and that of EP/3CNCs was slightly increased compared to pure EP. With the addition of NPCNCs, expanded char layers were formed, and the height increased differently as the amount of NPCNCs increased.

SEM was used to study the microscopic morphology of carbon residue. For pure EP and EP/3CNCs, there were many holes on carbon residue outer surface because of gas ejection, which made it difficult to play a role of heat insulation and oxygen insulation (Shi et al. 2018). EP/NPCNC composites formed a denser char with fewer pores, which could

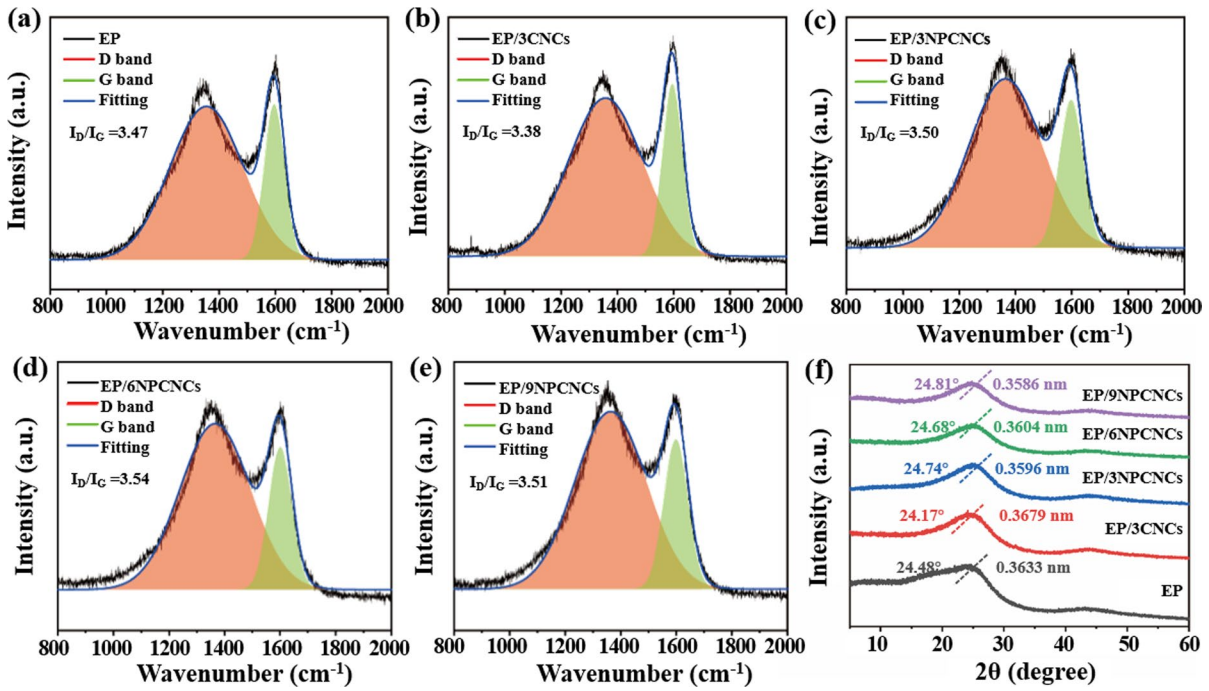

Fig. 7 Raman spectra of (**a**) EP, (**b**) EP/3CNCs, (**c**) EP/3NPCNCs, (**d**) EP/6NPCNCs, (**e**) EP/9NPCNCs and (**f**) XRD pattern of carbon residue after CCT

effectively inhibited heat and mass transfer, avoiding further combustion and improving flame retardancy. As can be seen from Fig. 6(d), the inner surface of the EP/6NPCNCs was denser, and there were vesicular substances, which may be due to the formation of pyrophosphate or metaphosphate (Feng et al. 2018; Xu et al. 2023). In addition, the EDS results showed that C and O elements were detected in the carbon residue of pure EP. For EP/9NPCNCs, there existed C, O and P elements, while not contained N element. This indicated that nitrogen containing gases (N_2 and NH_3) (Zhu et al. 2020) were released during combustion, while phosphorus containing compounds played a role in the condensed phase of the char layer (Sui et al. 2020).

Raman was used to characterize the graphitization degree of carbon residue. The results showed that carbon residues showed two peaks as D band (1351 cm^{-1}, belonged to graphitized carbon) and G band (1595 cm^{-1}, belonged to amorphous carbon) (Wang et al. 2023a, b). The I_D/I_G ratios of carbon residue of EP, EP/3CNCs, EP/3NPCNCs, EP/6NPCNCs and EP/9NPCNCs were 3.47, 3.38, 3.50, 3.54 and 3.51, respectively. EP/9NPCNCs' I_D/I_G ratio was the highest, indicating that it had the smallest carbonaceous structure and the highest degree of graphitization. It showed that more stable carbon layers were formed during the combustion process, which can well insulate heat and oxygen, thereby inhibiting combustion, protecting the substrate, and improving fire safety.

The XRD patterns of the carbon residue were shown in Fig. 7(f). The carbon residue of pure EP and EP/3CNCs showed one wide diffraction peak at 24.48° and 24.17° with a crystal plane spacing of 0.3633 and 0.3679 nm, indicating the formation of graphitization during the combustion process (Yu et al. 2015). While the wide peaks of EP/3NPCNCs, EP/6NPCNCs and EP/9NPCNCs shifted to 24.74°, 24.68°, and 24.81° with crystal plane spacing of 0.3596, 0.3660, and 0.3586 nm, respectively. The results showed that the addition of NPCNCs was conducive to the formation of a denser semi-focal layer (Shao et al. 2018). The results were consistent with digital photographs of carbon residues.

The pyrolytic products and toxic gases generated during the degradation of EP and its composites were characterized by TG-FTIR. 3D

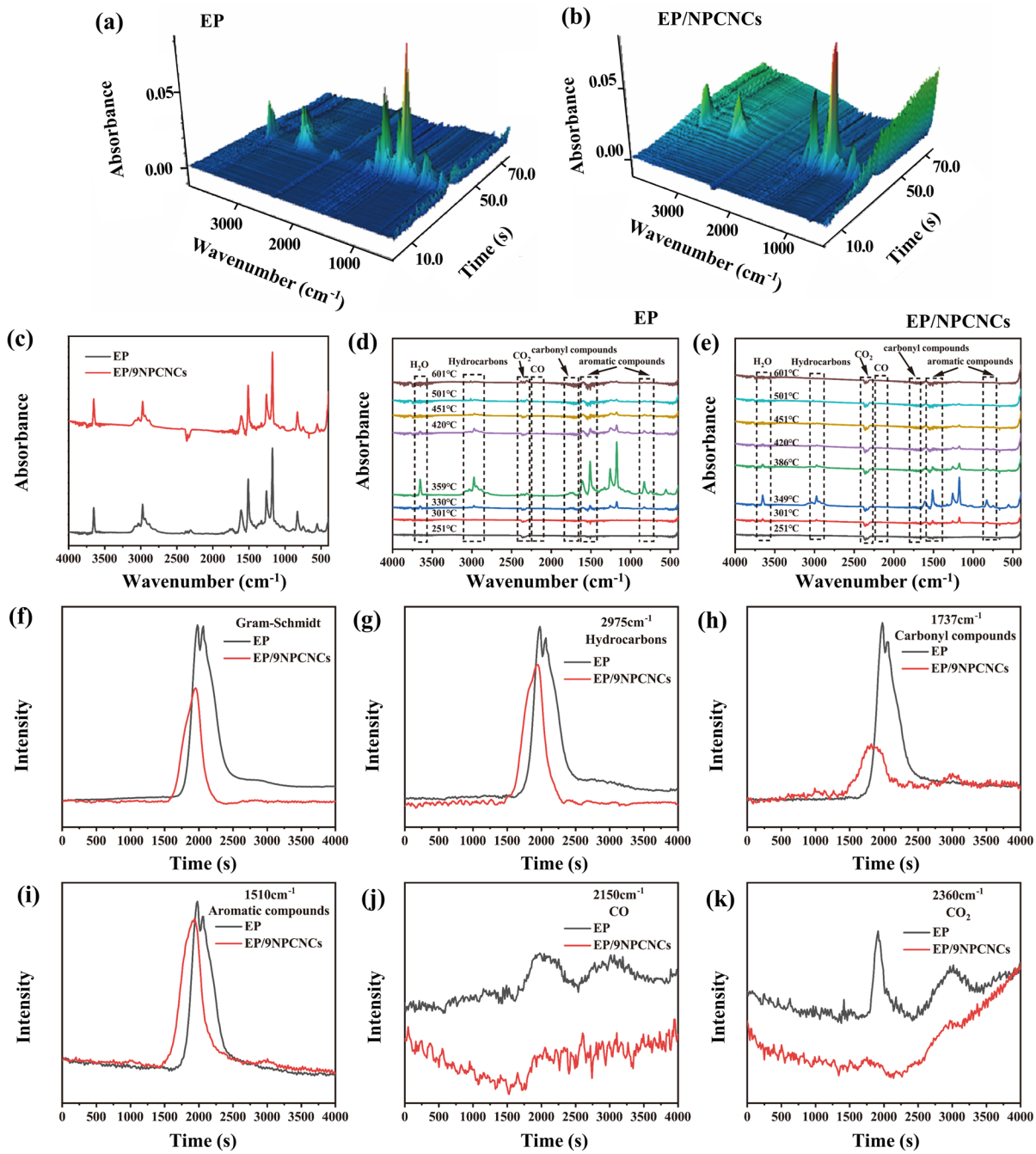

Fig. 8 (**a**-**b**) 3D TG-FTIR and (**c**) FTIR spectra at the maximum decomposition rate; FTIR spectra of pyrolysis products at different temperature: (**d**) EP; (**e**) EP/9NPCNCs; (**f**) total pyrolysis products; (**g**) Hydrocarbons; (**h**) carbon dioxide; (**i**) aromatic compounds; (**j**) CO and (**k**) CO_2

TG-FTIR (Fig. 8(a-b)) and FTIR (Fig. 8(c)) spectra at the maximum decomposition rate showed that the absorption intensity of EP/9NPCNCs reduced compared to that of pure EP. And the infrared spectra of gaseous decomposition products of EP composites mainly included water

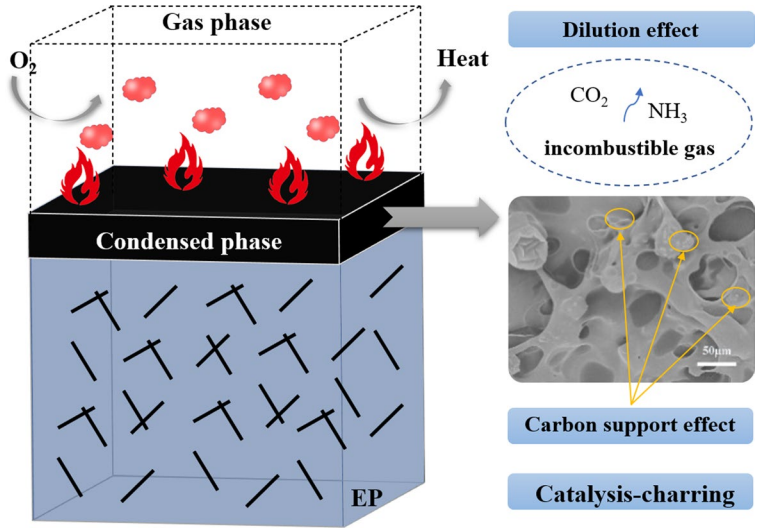

Fig. 9 The flame-retardant mechanism

or phenol (3500–4000 cm^{-1}), hydrocarbons (2750–3200 cm^{-1}), CO_2 (2200–2400 cm^{-1}), carbonyl compounds (1750–1900 cm^{-1}), and aromatic ring containing compounds (1250–1600 cm^{-1}, 600–1000 cm^{-1}) (Qiu et al. 2017). Compared with pure EP in Fig. 8(f), the absorption intensity of EP/9NPCNCs was shorter and thinner, indicating that NPCNCs had an inhibitory effect on the release of precipitated gas in the thermal decomposition process of EP composites (Fu et al. 2022; Li et al. 2022). The main sources of smoke particles during combustion were organic volatile products, such as hydrocarbons, carbonyls, and aromatic compounds (Li et al. 2020; Liu et al. 2021). The absorption intensity at 2975 cm^{-1} (hydrocarbons), 1737 cm^{-1} (carbonyl compounds), 1510 cm^{-1} (aromatic compounds), 2150 cm^{-1} (CO) and 2360 cm^{-1} (CO_2) of EP/9NPCNCs were significantly reduced (Hong

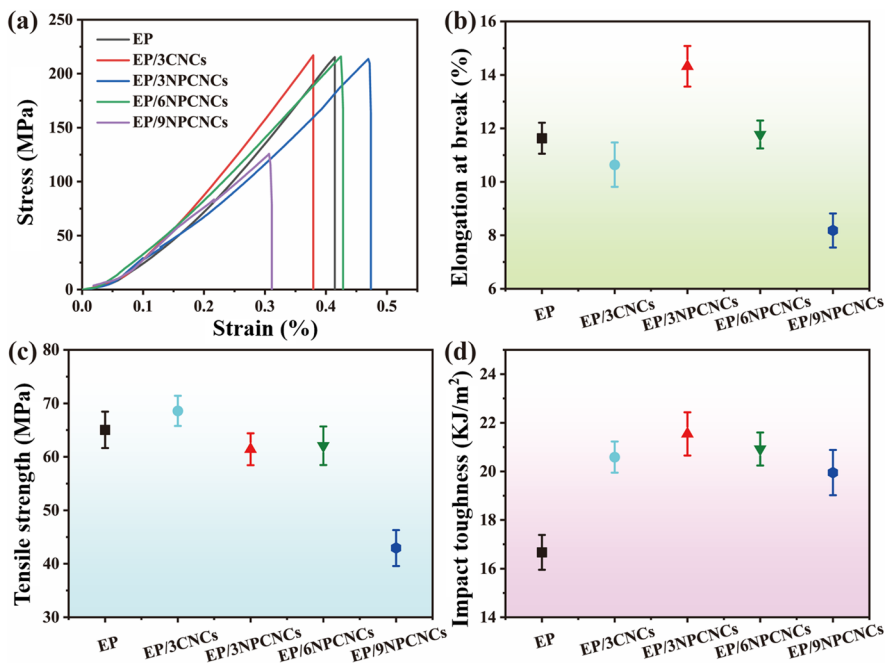

Fig. 10 Typical tensile stress–strain curves

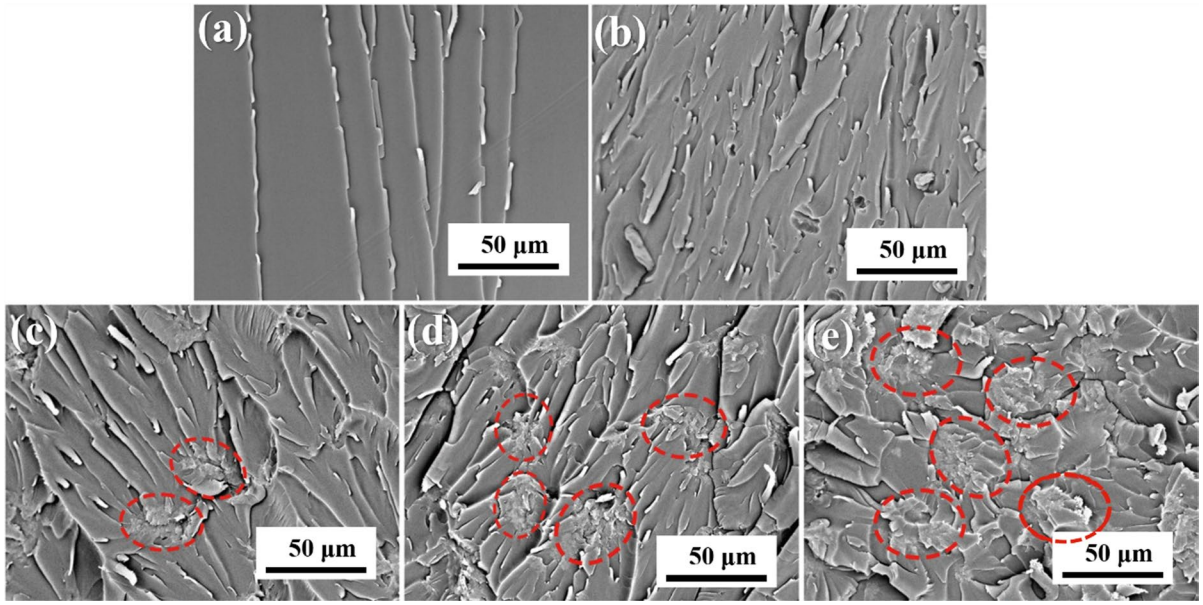

Fig. 11 SEM images of cryofracture sections: (**a**) EP; (**b**) EP/3CNCs; (**c**) EP/3NPCNCs; (**d**) EP/6NPCNCs and (**e**) EP/9NPCNCs

et al. 2022) compared with that of pure EP. The reduction of these volatiles helped to suppress the release of smoke, which was conducive to improving fire safety (Liang et al. 2023; Rao et al. 2023).

The mechanism was proposed (Fig. 9). The introduction of phosphorus and nitrogen elements into CNCs can endow excellent flame retardancy to EP. CNCs served as templates and carbon to provide support and source for carbon residue; The addition of PA containing phosphorus compound can promote the carbonization and dehydration of CNCs and EP matrix during combustion, thereby greatly improving the yield of carbon residue; Nitrogen-containing PANI can produce incombustible gases during combustion. In summary, in the condensed phase, due to the catalytic and dehydration carbonization effects of phosphorus containing compounds, as well as the good support effect of fibrous CNC templates, EP composite materials generated a more stable and dense char layer during combustion (Wang et al. 2022, 2024). Moreover, phosphorus and nitrogen element collaborative improved carbon residue stability, avoided further oxidation, prevented the collapse, as well as the formation of pores and cracks. The char layer acted as a physical barrier to reduce mass and heat transfer and prevented volatiles from escaping. In the gas phase, non combustible gases such as NH_3 and CO_2 generated by NPCNCs diluted the concentration of combustible gases and oxygen, thereby preventing combustion.

Table 3 Mechanical property data of EP composites

Samples	Elongation at break (%)	Tensile strength (MPa)	Impact toughness (kJ/m^2)
EP	11.63 ± 3.41	65.05 ± 0.58	16.67 ± 0.72
EP/3CNCs	10.64 ± 2.81	68.59 ± 0.83	20.59 ± 0.64
EP/3NPCNCs	14.32 ± 2.99	61.41 ± 0.73	21.54 ± 0.89
EP/6NPCNCs	11.77 ± 3.60	62.07 ± 0.52	20.92 ± 0.68
EP/9NPCNCs	8.18 ± 3.36	42.94 ± 0.64	19.95 ± 0.93

Mechanical performance

The mechanical properties of EP composites were explored (Fig. 10). Pure EP has an elongation at break (EB) of 12.37% and a tensile strength (TS) of 65.01 MPa. For EP/3CNCs the EB value was slightly decreased and TS value was slightly increased, indicating the tensile properties remained basically. Compared to pure EP, the tensile properties of EP/3NPCNCs and EP/6NPCNCs increased. And EB value of EP/3NPCNCs increased to 14.32%, which was 23.13% higher than that of pure EP. While the EB and TS values of EP/9NPCNCs decreased significantly. The impact toughness (IT) of pure EP was 16.67 kJ/m^2. After adding CNCs and NPCNCs, the IT value of EP composites increased by different degrees. For EP/3NPCNCs, the IT value was 21.54 kJ/m^2, which increased by 29.21% compared to pure EP (Table 3).

The cross-section of the composite was characterized by SEM to study the dispersion characteristics of prepared flame retardant in EP (Fig. 11). SEM results showed that pure EP had a typical brittle fracture behavior, with neat and smooth cross sections (Jiang et al. 2023). The cross-section of EP/3CNCs became rough and has no obvious agglomeration phenomenon in the cross-section. When NPCNCs amount was added, the roughness of the fracture surface increased, and certain aggregates appeared in the fracture surface. Due to its strong hydrogen bonding characteristics, NPCNCs tended to aggregate in the matrix, which led to the formation of a permeable network, resulting in a significant increase in roughness and more pronounced wrinkles.

Conclusion

Phosphorus nitrogen modified CNC hybrid flame retardant was successfully prepared by ice bath polymerization. The effect of prepared NPCNCs on the flame retardant and mechanical properties of EP composite was investigated. Combined with TEM, XRD, FTIR, XPS, it was proved that NPCNCs were successfully synthesized and exhibited a fibrous structure with a rough surface. NPCNCs endowed EP excellent flame retardancy. Compared with pure EP, the THR, PHRR, TSP, and PSPR values of EP/6NPCNCs were reduced by 27.27%, 43.34%, 70.21%, and 66.67%, respectively. The addition of NPCNCs allowed EP to generate a denser carbon layer during the combustion process, thereby blocking the release of oxygen, heat, and smoke. In the gas phase, on the one hand NPCNCs generated incombustible gases to dilute combustible gases, and on the other hand the addition of NPCNCs inhibited the release of volatile combustible compounds such as hydrocarbons, carbon groups, and aromatic molecules, thereby reducing the release of heat and smoke. In addition, NPCNCs basically maintained the mechanical properties of EP.

Acknowledgments Not applicable

Author contributions Weihua Meng: Conceptualization, Methodology, Visualization, Project administration, Chang Wang and Hang Di: Writing—Original Draft, Data curation; Shuo Ren: Data curation, Formal analysis; Jianing Wu: Resources, Visualization; Xuyang Sun: Data curation, Resources; Lide Fang: Conceptualization, Methodology; Xiangjie Kong: Project administration; Jianzhong Xu: Visualization, Project administration; All authors reviewed the manuscript.

Funding This work was supported by the Natural Science Foundation of Hebei Province [grant numbers E2022201030]; Funded by Science Research Project of Hebei Education Department [grant numbers QN2023020]; Key projects supported by selected postdoctoral candidates in Hebei Province [grant numbers B2022005001]; the Open Project Program of Fujian Key Laboratory of Special Intelligent Equipment Measurement and Control, Fujian Special Equipment Inspection and Research Institute, China [grant numbers FJIES2023KF11]; the National Natural Science Foundation of China [grant numbers 62173122]; and Post-graduate's Innovation Fund Project of Hebei University [grant numbers HBU2023SS035].

Data availability No datasets were generated or analysed during the current study.

Declarations

Ethics approval and consent to participate Not applicable.

Consent for publication The manuscript has been approved by all authors.

Competing interests The authors declare no competing interests.

References

Bhoite SP, Kim J, Jo W et al (2021) Expanded polystyrene beads coated with intumescent flame retardant material to

achieve fire safety standards. Polymers-Basel 13(16):2662. https://doi.org/10.3390/polym13162662
Chen L, Wang Y-Z (2010) A review on flame retardant technology in China. Part 1: development of flame retardants. Polym Advan Technol 21(1):1–26. https://doi.org/10.1002/pat.1550
Chen J, Zhu Z, Zhang H et al (2021) Wood-derived nanostructured hybrid for efficient flame retarding and electromagnetic shielding. Mater Des 204:109695. https://doi.org/10.1016/j.matdes.2021.109695
Chen Q, Wang S, Li S et al (2023a) Highly efficient phosphorous-containing flame retardant for transparent epoxy resin with good mechanical properties. J Polym Res 30(1):32. https://doi.org/10.1007/s10965-022-03398-4
Chen X, Piao J, Dong H et al (2023) Organic phosphoric acid doped polyaniline-coupled g-C_3N_4 for enhancing fire safety of intumescent flame-retardant epoxy resin. Macromol Rapid Comm 44(12). https://doi.org/10.1002/marc.202300071
Cheng L, Wang J, Qiu S et al (2021) Supramolecular wrapped sandwich like SW-Si_3N_4 hybrid sheets as advanced filler toward reducing fire risks and enhancing thermal conductivity of thermoplastic polyurethanes. J Colloid Interface Sci 603:844–855. https://doi.org/10.1016/j.jcis.2021.06.153
Du W, Ge X, Huang H et al (2022) Fabrication of high transparent, mechanical strong, and flame retardant waterborne polyurethane composites by incorporating phosphorus-silicon functionalized cellulose nanocrystals. J Appl Polym Sci 139(3):e51496. https://doi.org/10.1002/app.51496
Fang F, Huo S, Shen H et al (2020) A bio-based ionic complex with different oxidation states of phosphorus for reducing flammability and smoke release of epoxy resins. Compos Commun 17:104–108. https://doi.org/10.1016/j.coco.2019.11.011
Fang Y, Sun W, Li J et al (2021) Eco-friendly flame retardant and dripping-resistant of polyester/cotton blend fabrics through layer-by-layer assembly fully bio-based chitosan/phytic acid coating. Int J Biol Macromol 175:140–146. https://doi.org/10.1016/j.ijbiomac.2021.02.023
Feng Y, He C, Wen Y et al (2018) Superior flame retardancy and smoke suppression of epoxy-based composites with phosphorus/nitrogen co-doped graphene. J Hazard Mater 346:140–151. https://doi.org/10.1016/j.jhazmat.2017.12.019
Fu C, Xu X, Yin G-Z et al (2022) Surface engineering for cellulose as a boosted Layer-by-Layer assembly: excellent flame retardancy and improved durability with introduction of bio-based "molecular glue." Appl Surf Sci 585:152550. https://doi.org/10.1016/j.apsusc.2022.152550
He J, Sun Z, Chen Y et al (2022) Grafting cellulose nanocrystals with phosphazene-containing compound for simultaneously enhancing the flame retardancy and mechanical properties of polylactic acid. Cellulose 29(11):6143–6160. https://doi.org/10.1007/s10570-022-04647-x
Hong J, Wu T, Wang X et al (2022) Copper-catalyzed pyrolysis of halloysites@polyphosphazene for efficient carbonization and smoke suppression. Compos Part B-Eng 230:109547. https://doi.org/10.1016/j.compositesb.2021.109547
Huang C, Zhao Z-Y, Deng C et al (2021) Facile synthesis of phytic acid and aluminum hydroxide chelate-mediated hybrid complex toward fire safety of ethylene-vinyl acetate copolymer. Polym Degrad Stabil 190:109659. https://doi.org/10.1016/j.polymdegradstab.2021.109659
Huo S, Song P, Yu B et al (2021) Phosphorus-containing flame retardant epoxy thermosets: Recent advances and future perspectives. Prog Polym Sci 114:101366. https://doi.org/10.1016/j.progpolymsci.2021.101366
Jiang G, Xiao Y, Qian Z et al (2023) A novel phosphorus-, nitrogen- and sulfur-containing macromolecule flame retardant for constructing high-performance epoxy resin composites. Chem Eng J 451:137823. https://doi.org/10.1016/j.cej.2022.137823
Kandola BK, Magnoni F, Ebdon JR (2022) Flame retardants for epoxy resins: application-related challenges and solutions. J Vinyl Addit Technol 28(1):17–49. https://doi.org/10.1002/vnl.21890
Kumar A, Rao KM, Han SS (2017) Development of sodium alginate-xanthan gum based nanocomposite scaffolds reinforced with cellulose nanocrystals and halloysite nanotubes. Polym Test 63:214–225. https://doi.org/10.1016/j.polymertesting.2017.08.030
Li N, Liu L, Yang F (2014) Highly conductive graphene/PANi-phytic acid modified cathodic filter membrane and its antifouling property in EMBR in neutral conditions. Desalination 338:10–16. https://doi.org/10.1016/j.desal.2014.01.019
Li W-X, Zhang H-J, Hu X-P et al (2020) Highly efficient replacement of traditional intumescent flame retardants in polypropylene by manganese ions doped melamine phytate nanosheets. J Hazard Mater 398:123001. https://doi.org/10.1016/j.jhazmat.2020.123001
Li X-L, Shi X-H, Chen M-J et al (2022) Biomass-based coating from chitosan for cotton fabric with excellent flame retardancy and improved durability. Cellulose 29(9):5289–5303. https://doi.org/10.1007/s10570-022-04566-x
Liang J, Yang W, Yuen ACY et al (2023) A novel green IFR system: design of a self-assembled peanut shell-based flame retardant and its fire performance in EP. Prog Org Coat 174:107277. https://doi.org/10.1016/j.porgcoat.2022.107277
Liu L, Xu Y, Pan Y et al (2021) Facile synthesis of an efficient phosphonamide flame retardant for simultaneous enhancement of fire safety and crystallization rate of poly (lactic acid). Chem Eng J 421:127761. https://doi.org/10.1016/j.cej.2020.127761
Lou Y, Ma H, Su Y et al (2023) Cavity expansion and nanohybrid copper phytate@halloysite coated with polyphosphazene for reducing smoke release and fire hazard of epoxy resin. Appl Clay Sci 231:106756. https://doi.org/10.1016/j.clay.2022.106756
Luo H, Rao W, Zhao P et al (2020) An efficient organic/inorganic phosphorus-nitrogen-silicon flame retardant towards low-flammability epoxy resin. Polym Degrad Stabil 178:109195. https://doi.org/10.1016/j.polymdegradstab.2020.109195
Meng W, Dong Y, Li J et al (2020) Bio-based phytic acid and tannic acid chelate-mediated interfacial assembly of $Mg(OH)_2$ for simultaneously improved flame retardancy, smoke suppression and mechanical properties of PVC. Compos Part B-Eng 188:107854. https://doi.org/10.1016/j.compositesb.2020.107854

Meng W, Song Y, Zhai K et al (2022) Assembling MXene with bio-phytic acid: Improving the fire safety and comprehensive properties of epoxy resin. Polym Test 110:107564. https://doi.org/10.1016/j.polymertesting.2022.107564

Mokhena TC, Sadiku ER, Ray SS et al (2022) Flame retardancy efficacy of phytic acid: an overview. J Appl Polym Sci 139(27):e52495. https://doi.org/10.1002/app.52495

Peng X, Liu Q, Wang D et al (2021) A hyperbranched structure formed by in-situ crosslinking of additive flame retardant endows epoxy resins with great flame retardancy improvement. Compos Part B-Eng 224:109162. https://doi.org/10.1016/j.compositesb.2021.109162

Qi Y, Hou Z, Xu S et al (2023) The flame retardant properties and mechanism of the composites based on DOPS and triazine-trione groups in epoxy resin. Polym Degrad Stabil 216:110482. https://doi.org/10.1016/j.polymdegradstab.2023.110482

Qiu S, Shi Y, Wang B et al (2017) Constructing 3D polyphosphazene nanotube@mesoporous silica@bimetallic phosphide ternary nanostructures via layer-by-layer method: synthesis and applications. Acs Appl Mater Interfaces 9(27):23027–23038. https://doi.org/10.1021/acsami.7b06440

Rao W, Tao J, Yang F et al (2023) Growth of copper organophosphate nanosheets on graphene oxide to improve fire safety and mechanical strength of epoxy resins. Chemosphere 311:137047. https://doi.org/10.1016/j.chemosphere.2022.137047

Shao Z-B, Zhang M-X, Li Y et al (2018) A novel multi-functional polymeric curing agent: synthesis, characterization, and its epoxy resin with simultaneous excellent flame retardance and transparency. Chem Eng J 345:471–482. https://doi.org/10.1016/j.cej.2018.03.142

Shi Y-Q, Fu T, Xu Y-J et al (2018) Novel phosphorus-containing halogen-free ionic liquid toward fire safety epoxy resin with well-balanced comprehensive performance. Chem Eng J 354:208–219. https://doi.org/10.1016/j.cej.2018.08.023

Sui Y, Qu L, Dai X et al (2020) A green self-assembled organic supermolecule as an effective flame retardant for epoxy resin. Rsc Adv 10(21):12492–12503. https://doi.org/10.1039/d0ra00072h

Suo Y, Gao W, Chen Z et al (2022) Surface modification of cellulose nanocrystal and its applications in flame retardant epoxy resin. J Appl Polym Sci 139(28):e52617. https://doi.org/10.1002/app.52617

Wang P-J, Liao D-J, Hu X-P et al (2019) Facile fabrication of biobased P-N-C-containing nano-layered hybrid: Preparation, growth mechanism and its efficient fire retardancy in epoxy. Polym Degrad Stabil 159:153–162. https://doi.org/10.1016/j.polymdegradstab.2018.11.024

Wang Y, Liu L, Ma L et al (2022) Transparent, flame retardant, mechanically strengthened and low dielectric EP composites enabled by a reactive bio-based P/N flame retardant. Polym Degrad Stab 204:110106. https://doi.org/10.1016/j.polymdegradstab.2022.110106

Wang C, Huo S, Ye G et al (2023a) A P/Si-containing polyethylenimine curing agent towards transparent, durable fire-safe, mechanically-robust and tough epoxy resins. Chem Eng J 451:138768. https://doi.org/10.1016/j.cej.2022.138768

Wang Y, Ma L, Yuan J et al (2023b) A green flame retardant by elaborate designing towards multifunctional fire-safety epoxy resin composites. React Funct Polym 191:105677. https://doi.org/10.1016/j.reactfunctpolym.2023.105677

Wang Y, Zhang Y, Ma L et al (2024) Facile synthesis of phosphorus-containing benzotriazole flame retardant for enhancement of mechanical and fire properties of epoxy resins. Eur Polym J 202:112610. https://doi.org/10.1016/j.eurpolymj.2023.112610

Xiao Y, Mu X, Chen S et al (2023) Biomass-derived polyphosphazene toward simultaneously enhancing the flame retardancy and mechanical properties of epoxy resins. Chemosphere 311:137058. https://doi.org/10.1016/j.chemosphere.2022.137058

Xu Y, Yan C, Du C et al (2023) High-strength, thermal-insulating, fire-safe bio-based organic lightweight aerogel based on 3D network construction of natural tubular fibers. Compos Part B-Eng 261:110809. https://doi.org/10.1016/j.compositesb.2023.110809

Yang Y, Li Z, Wu G et al (2022) A novel biobased intumescent flame retardant through combining simultaneously char-promoter and radical-scavenger for the application in epoxy resin. Polym Degrad Stabil 196:109841. https://doi.org/10.1016/j.polymdegradstab.2022.109841

Yu B, Shi Y, Yuan B et al (2015) Enhanced thermal and flame retardant properties of flame-retardant-wrapped graphene/epoxy resin nanocomposites. J Mater Chem A 3(15):8034–8044. https://doi.org/10.1039/c4ta06613h

Zeng F, Qin Z, Chen Y et al (2021) Constructing polyaniline nanowire arrays as efficient traps on graphene sheets to promote compound synergetic effect in the assembled coating for multifunctional protective cotton fabrics. Chem Eng J 426:130819. https://doi.org/10.1016/j.cej.2021.130819

Zhang Z, Wu W, Zhang M et al (2017) Hydrothermal synthesis of $4ZnO{\bullet}B_2O_3{\bullet}H_2O$/RGO hybrid material and its flame retardant behavior in flexible PVC and magnesium hydroxide composites. Appl Surf Sci 425:896–904. https://doi.org/10.1016/j.apsusc.2017.07.101

Zhang S, Chen H, Zhang Y et al (2020) Flame retardancy of high-density polyethylene composites with P,N-doped cellulose fibrils. Polymers-Basel 12(2):336. https://doi.org/10.3390/polym12020336

Zhang Y, Yu H-Y, Dong Y et al (2023) Facile strategy to design a cellulose nanocrystal-based nanocomposite fire retardant with strong smoke suppression efficiency. Acs Sustain Chem Eng 11(35):12983–12991. https://doi.org/10.1021/acssuschemeng.3c02458

Zhi M, Yang X, Fan R et al (2022) A comprehensive review of reactive flame-retardant epoxy resin: fundamentals, recent developments, and perspectives. Polym Degrad Stabil

201:109976. https://doi.org/10.1016/j.polymdegradstab.2022.109976

Zhou Z, Yang Y, Han Y et al (2017) In situ doping enables the multifunctionalization of templately synthesized polyaniline@cellulose nanocomposites. Carbohyd Polym 177:241–248. https://doi.org/10.1016/j.carbpol.2017.08.136

Zhu M, Liu L, Wang Z (2020) Iron-phosphorus-nitrogen functionalized reduced graphene oxide for epoxy resin with reduced fire hazards and improved impact toughness. Compos Part B-Eng 199:108283. https://doi.org/10.1016/j.compositesb.2020.108283